International Journal of Multiphysics
Volume 19, No. 1, 2025
ISSN: 1750-9548

DYNAMICS PROPERTIES OF HOLE DEFECT ON MESOSCOPIC 2D SYSTEM

Sayhi Mostefa [(1)] , Bouchareb Sansabilla[(1)], Bouateli Mohamed [(2)], Tigrine Rachid [(1,2)]

[1] Laboratory of energy, environment and information systems, Ahmed Draya Adrar University Algeria
[2]Laboratory of Quantum Physics and Chemistry, University Mouloud Mammeri of TiziOuzou, Algeria.

Corresponding author:* mostefa.sayhi@univ-adrar.edu.dz
sansabilla123@gmail.com
tigriner@univ-adrar.edu.dz
tigriner@yahoo.fr

Received: 12/6/2024 Accepted: 14/03/2025 Published: 28/04/2025

Abstract.

We present a study of the dynamic phenomena at the inhomogeneous surface crystalline. The breakdown of translation symmetry induced by the inhomogeneity, gives rise to localized modes at its neighbourhood. The formalism of the matching method, the Newton equation and Green function are used to calculate the Rayleigh branches and associate state densities. The numerical results are presented in a large band of scattering energies. This illustrates theoretically the variation of localized phonons and their spectra of states densities for the softening, homogeneous and the hardening elastic constants of the neighbourhood of the perturbed domain. The coherent coupling between these localized phonons induced by the defect and the travelling modes of the perfect waveguide lead to Fano resonances at the state density spectra and Rayleigh dispersion branches.

Keywords: hole defect; matching method; Fano resonances; vibrational properties; state density
PACS: 61.46. +w ; 68.65.+g

1. Introduction

The scattering and localization phenomena of several systems with defects shows intriguing useful properties and they are more recent interest, [1-2].They are currently the subjects of active research because of their interest for high technology nanometric devices.

The inhomogeneities in the structure scatter the elastic waves of the unperturbed lattice, which can be considered as a waveguide. The resonances in the scattering spectra for a waveguide containing perturbed domains are a signature of the localization effects in the neighborhood of the perturbed domain.

There are strong similarities between electronic and vibrational scattering of point of view mathematical formalism, we just replace the Schrödinger equation by the Newton dynamical equation. The scattering of the vibrational waves is more complicated. Also its complexity in contrast with coherent electron transport is attributed to the vector character of the vibrational fields.

There are several theoretical methods to deal with the effects of different type of defects. The matching method that we employ in this work has previously been extended with success to study the scattering of elastic waves at isolated nanostructures in quasi-one-dimensional disordered systems, The specific advantage of the matching method, compared to other methods such as the cluster numerical approach, and besides being transparent at all stages of the calculation, is that it gives an exact and rigorous analytical formulation of the vibrational field displacements in the limit to infinity. There are no numerical approximations [3-6].

In this work, we present the study relating to the vibrational properties based on the matching method [7-9] associated to Green functions, in a 2D system with schoty defect. Recently, a similar study was presented by B. Djafari-Rouhani and *al* [10], in the case of polymers (a chain) adsorbed on a surface.

The paper is organised as follows. In section.1 we present the structural model and the dynamic vibration of the perfect wave guides. In section.2. we give the dynamical properties of the perturbed domain. In section.3, we describe the Green functions formalism, used for the calculation of the state density associated to localized phonons. In sec.4 some numerical results are presented, for three cases system parameters, respectively the softening, homogeneous and hardening and general conclusions.

International Journal of Multiphysics
Volume 19, No. 1, 2025
ISSN: 1750-9548

1. Structural model and the dynamical properties of the perfect wave guide

Our structural model is presented in Fig.1; it is crystalline surface with schoty defect (grey area). Far from the perturbed domain they are the perfect region.

The interaction in the perfect region, between the nearest and next nearest neighbour is represented respectively by elastic constant k_1 and k_2. In contrast, in the perturbed zone, these constants are labelled k_{1d} and k_{2d}. For simplicity, we take the same distance $\boldsymbol{a}$ between all adjacent sites in the different Cartesian directions.

In order to calculate the normalised frequencies in the system, we defined the following ratios:

$$r=k_2/k_1,\ r_{1d}=k_{,1}/k_1 \text{ and } r_{2d}=k_{,2}/k_1 \qquad (1)$$

In the harmonic approximation [11], the equation of motion of an atom at site l is given by:

$$\omega^2 m(l)U_\alpha(l)=-\Sigma_{l'\neq l}\Sigma_\beta k(l,l')r_\alpha.r_\beta/d^2\,[u_\beta(l)-u_\beta(l')] \qquad (2)$$

The indices α and β denote Cartesian co-ordinates, m ≡ m(l) is the mass, and $u_\alpha(l)$ is the corresponding displacement vector vibration, of the l atom. The radius vector **r** between the atomic sites at l and l', has Cartesian components r_α , and d = $|\mathbf{r}|$. The force constant between the two sites is $k(l,l')$, so that $k(l,l')=k_1$ and $k(l,l')=k_2$ respectively for nearest and next nearest neighbours.

The dynamics of atomic sites may be described by the travelling wave solutions of Eq. (2).

Suppose that l and l' are in side the perfect wave-guide, as in Fig.1. The solutions to Eq. (2) for the wave-guide are obtained from:

$$[\Omega^2 I - D(\eta, r)]|U\rangle=0 \qquad (3)$$

Ω is a dimensionless frequency given by $\Omega^2=\omega^2/\omega_0^2$, where ω_0 is a characteristic lattice frequency, $\omega_0^2=k_1/m$, and D(η, r) is the dynamic matrix characteristic of the perfect wave guide lattice. I is the corresponding unit matrix. η : is the phase factor.

In the configuration described by Fig.1, D is reduced a two by two matrix, for the atomic site per unit cell and two degrees of freedom per site. |U> is the corresponding vector for a column of the perfect wave-guide.

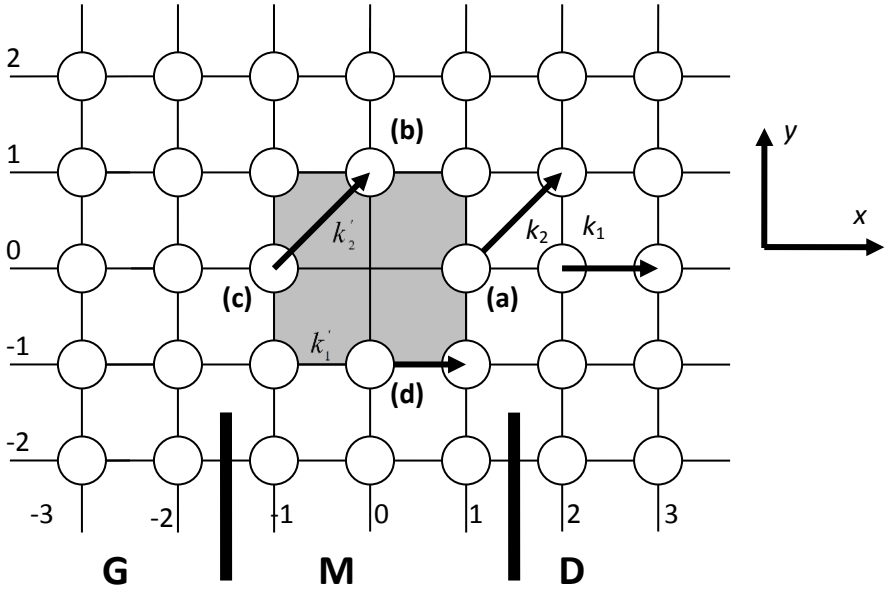

Fig.1: Schematic representation of 2D crystallographic waveguide with configuration hole. The perturbed domain is the grey area, with the content of the defects force constants

The evanescent and propagating vibrational modes in perfect waveguide are described by the phase factor doublets: $\{\eta,\eta^{-1}\}$.

With the matching method applied to Eq.(3), the evanescent modes are obtained when $|\eta|<1$, and the propagating modes are determined by the condition $|\eta|=1$.

Consequently, solutions are obtained when the determinant of $[\Omega^2 I - D(\eta, r)]$ vanishes. The determinant give a secular equation of degrees 4 of η. Its is expressed in polynomial forms by $\sum_{i=0}^{4} A_i \eta^i = 0$, (the term A_i of the summation depend on (Ω, r)). The hermitic nature of the matrix dynamics of the perfect region implicates that the both phase factors η and η^{-1} verify symmetrically the polynomials forms above.

The summation gives a maximum two solutions for η. In Fig.2a and Fig.2b shows the evolution of the phase factor as a function of the incident phonon frequency for each vibrating mode characterizing the waveguide. One can find two types of phase the new propagating frequency ranges of all two waveguide modes.

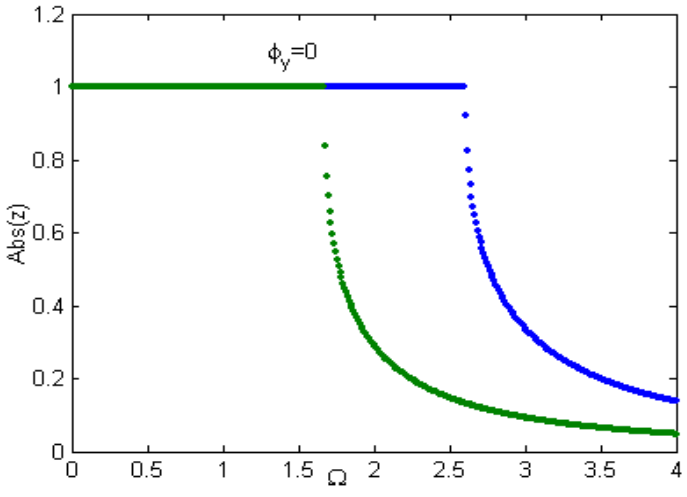

Fig.2a: The phase factor evolution as a function of the dimensionless frequency and the elastic constant for the waveguide eigenmodes; for incidence .φ_y= 0

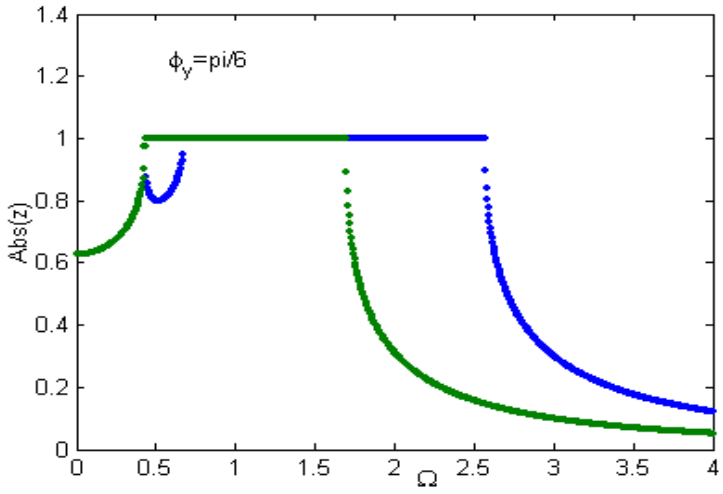

Fig.2b : The phase factor evolution as a function of the dimensionless frequency and the elastic constant for the waveguide eigenmodes; for incidence .φ_y= π/6

International Journal of Multiphysics
Volume 19, No. 1, 2025
ISSN: 1750-9548

2. Dynamical properties at the inhomogeneity:

The Cartesian component u_α, of the displacements field for an atom localised in the matching domain, before perturbed domain (see Fig.1) can be written [11-15]:

$$u_\alpha(n,m)=\sum_{i=1}^{6}[\eta(i)]^{n}R_i^{+}\rho(\alpha,i) \quad (4)$$

Whereas for sites in second matching domain (after the perturbed domain), is described by:

$$u_\alpha(n',m')=\sum_{i=1}^{6}[\eta(i')]^{-n}R_{i'}\rho(\alpha,i') \quad (5)$$

In equations (4) and (5), the quantities R_i^{+} and $R_{i'}$ represent unit vectors. They span the space of the solutions corresponding to the set $\{\eta, \eta^{-1}\}$. The coefficients $\rho(\alpha,i)$ and $\rho(\alpha,i')$ identify the relative weighting factors associated with the atomic displacements u_α and u'_α .

The set of irreducible sites in the defect region and the minimum representative set of sites in the matching regions of the system are chosen as indicated in Fig.1. Denoting by $|R\rangle$ the basis vector in the constructed space, using equations (4) and (5), and after the transformations connecting the two vectors $|R\rangle$ and $|U\rangle$, we obtain a square linear homogeneous of equations:

$$[\Omega^2 I - D(\eta, r, r_{1d}, r_{2d,} \Omega)]|U,R>=0 \quad (6)$$

Where I is the matrix unity, $i\in\{1,2\}$. D is a characteristic matrix calculated following the matching procedure. The dimensions of this square matrix are characteristic, for completeness, of an irreducible set of atomic sites at the surface boundary, and of the size of the constructed Hilbert space for the matching domains, is the square matrix of 12 by 12 elements,.

The matching procedure provides a framework for the calculation of the localized modes and of the spectral densities at the surface [16-29]. By diagonalizing the matrix [D((r, r_{1d}, r_{2d}, η, Ω], we calculate the dispersion branches of the Rayleigh phonon modes. The essential characteristic of these modes is that they propagate in the direction high symmetry of

the system model and decrease on both sides of the inhomgeneity. One notes the resonance modes inside the bulk band and appearance of the new modes in the windows of the bandwidth. The curves of localized phonons are presented in Figs (3-5)

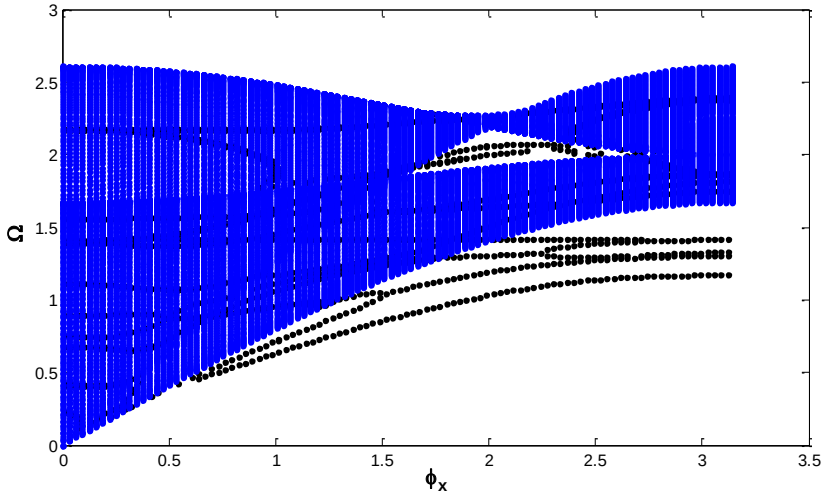

Fig.3: The Rayleigh phonon dispersion branches on the *hole* domain boundary, as a function of the wave vector φ_y, for homogeneous boundary elastic softening, r1d=0.6 and r2d=0.4

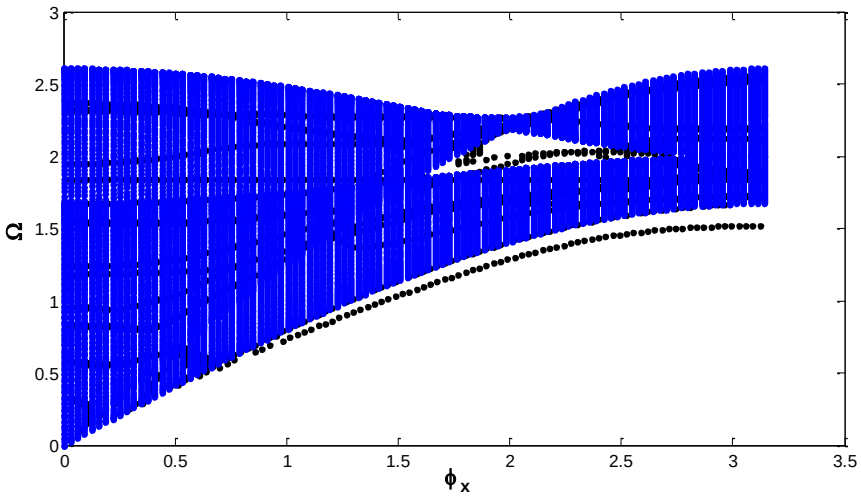

Fig.4: The Rayleigh phonon dispersion branches on the *hole* domain boundary, as a function of the wave vector φ_y, for homogeneous boundary elastic constants, r1d=1 and r2d=0.7

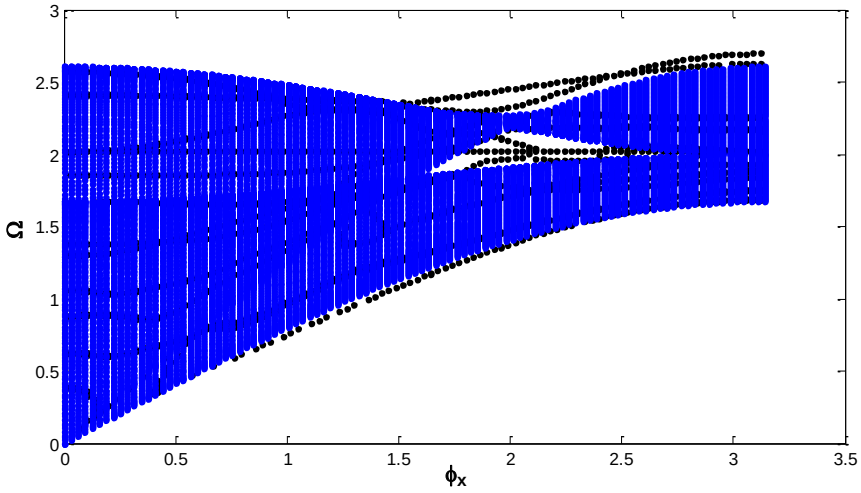

Fig.5: The Rayleigh phonon dispersion branches on the *hole* domain boundary, as a function of the wave vector φ_y, for hardening boundary elastic constants, r1d = 1.1 and r2d= 0.95.

3. State densities at the Behaviour of the schoty defect.

For completeness the calculated density of states (DOS) of the irreducible sites of the system model are presented via the Green functions associated to the matching method [11], it is expressed as:

$$G(\Omega^2 + i\varepsilon) = [\, D(\eta_2,\ \eta_3,\ e^{i\phi z},\ \Omega,\ r_0, r_1, r_2, r_3, r_4)\,]^{-1} \qquad (6)$$

The DOS per atomic site l, denoted as $\Xi_l(\Omega)$, is obtained as a sum over the trace of the spectral density matrix.

$$\Xi_l(\Omega) = \sum_{\alpha} \rho^{(l,l)}_{(\alpha,\alpha)}(\Omega) = -\frac{2\Omega}{\pi} \sum_{\alpha} \lim_{\varepsilon \to 0^+} \left\{ \mathrm{Im}\left[G^{ll}_{\alpha\alpha}\left(\Omega^2 + i\varepsilon\right) \right] \right\} \qquad (7)$$

The spectra presented on Figs. (6- 8) correspond to the localized DOS for perturbed sites, for different parameters of the system.

International Journal of Multiphysics
Volume 19, No. 1, 2025
ISSN: 1750-9548

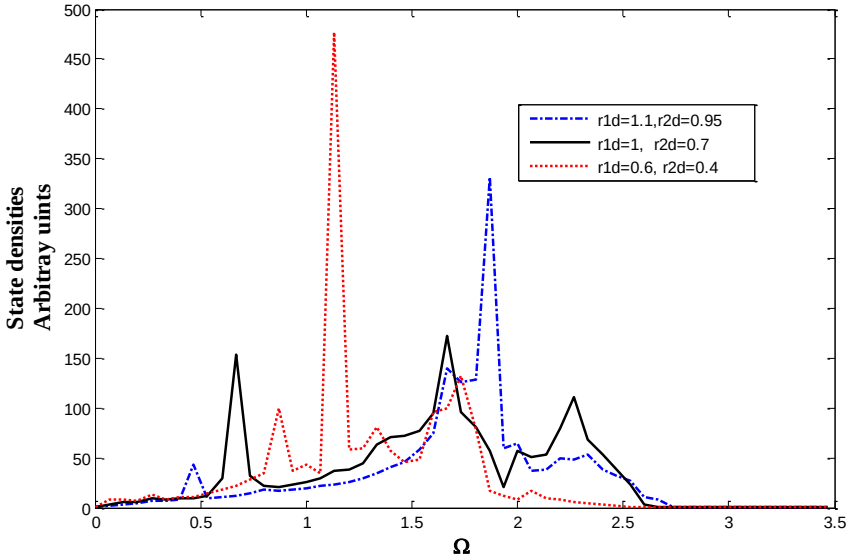

Fig6 : The density of states (DOS), for an atomic site (a) as function of the wave vector φ_y, the dimensionless frequencies Ω. For elastic softening, r1d=0.6 and r2d=0.4(doted-line), for homogeneous boundary (solid-line) r1d=1, r2d=07 and hardening boundary r1d = 1.1 and r2d= 0.95.(dashed doted –line).

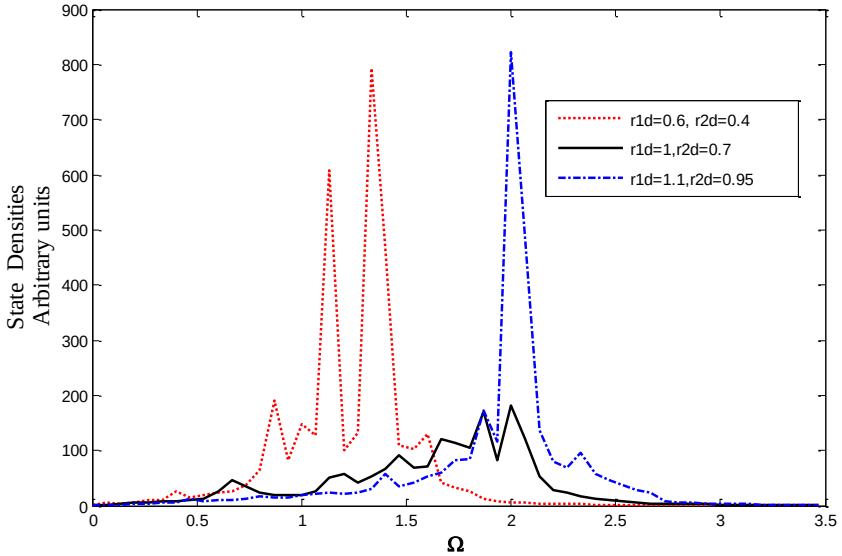

Fig7: The density of states (DOS), for an atomic site (b) as function of the wave vector φ_y, the dimensionless frequencies Ω. For elastic softening, r1d=0.6 and r2d=0.4(doted-line), for homogeneous boundary (solid-line) r1d=1, r2d=07 and hardening boundary r1d = 1.1 and r2d= 0.95.(dashed doted –line).

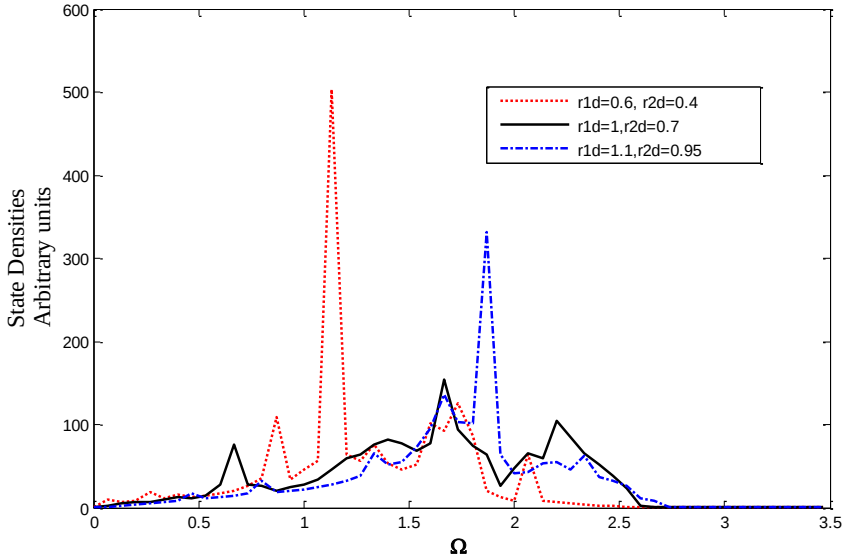

Fig.8: The density of states (DOS), for an atomic site (c) as function of the wave vector φ_y, the dimensionless frequencies Ω. For elastic softening, r1d=0.6 and r2d=0.4(doted-line), for homogeneous boundary (solid-line) r1d=1, r2d=07 and hardening boundary r1d = 1.1 and r2d= 0.95.(dashed doted –line).

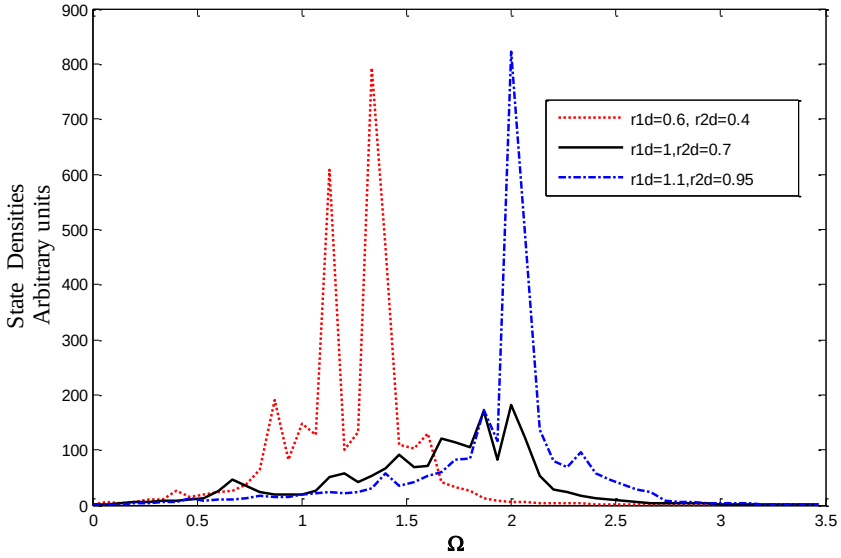

Fig.9: The density of states (DOS), for an atomic site (c) as function of the wave vector φ_y, the dimensionless frequencies Ω. For elastic softening, r1d=0.6 and r2d=0.4(doted-line), for homogeneous boundary (solid-line) r1d=1, r2d=07 and hardening boundary r1d = 1.1 and r2d= 0.95.(dashed doted –line).

4. Numerical results and discussion

The numerical results of the Rayleigh branches of localized phonons and their state densities at the perturbed domain are studied as function of dimensionless frequencies and the elastic constant of behavior of the defect on Fig.1. This analysis is carried out for three possibilities:

(*i*) $r_{1d}=r_1=1.0$, $r_{2d} = r_2=0.70$, (homogeneous case)

(*ii*) $r_{1d}=1.1 > r_1$, $r_{2d} =0.95 > r$, (hardening)

(*iii*) $r_{1d}=0.60<r_1$, $r_{2d} =0.40 < r$. (softening)

The dispersion relations of the localized phonons for numerical calculations are illustrated in a set of Figures [3, 4, 5]. They correspond respectively to cited previous cases respectively. In these figures, the modes outside the phonon band limits represent the dispersion curves of the phonon modes localized at the defect. They illustrate the breakdown of the translational symmetry induced by the presence of the lacuna. Several new Raleigh-like branches are induced at behavior of the inhomogeneity. In Fig.3a, corresponding to $r_{1d}=0.60<r_1$, $r_{2d} =0.40 < r$, the softening case, several acoustic Rayleigh branches appear alone below bulk subband of the system and two branches in window of Brillouin Zone (Z.B). In Fig.3b corresponding to the homogeneous case: $r_1=1.0$, $r_{2d} = r_2=0.70$ several acoustic modes disappear, leaving one mode at the perturbed domain.

One in Fig.3c, the hardening case is presented, the Rayleigh branches shifts to higher frequencies and two optical modes appear above (Z.B) and three modes induced in window of the bulk band. However the comportment of Rayleigh branches is sensible for the variation of the parameters of the system in the bulk and neighborhood of the hole.

The Fig.4 gives the state densities of atomic site (a), right of the hole, several resonance peaks appear on this curve related to Fano resonance. Its sensible to the variation of the ratio r1d and the r2d and shifts to higher frequencies for increasing values of previous ratios. In Figs.5, 6 and 7, we present the densities of states of atomic sites respectively (b), (c) and (d), in the frequency interval from 0 to 2.6. Same the previous case several peaks appear on their spectra, depending also of the parameters of the structure at the bulk and behavior of the inhomogeneity. Every curve is a signature of the nature and geometric defect and can be utilized as a probe in the non-destructive control.

5. Generals conclusions

In conclusion a hyperfine resonance structure is obtained that permits the analysis of the evolution of the dynamics at the schoty defect. The formalism presented is an analytical approach that is independent of the details of the nanostructure. This model shows the existence of localized Rayleigh-like modes induced by inhomogeneity. The presence of the defect lifts the degeneracy of the bulk phonon modes. The defect region generates the new branches of localized vibrational modes at its neighborhood. Further their number and their frequencies, depend strongly on the variation of elastic constants of the inhomogeneity. At this time, experimental or simulated data are not available for comparison. This model applies to acoustical studies at a macroscopic scale. Hence the possibility to test these theoretical results with an experiment model using scale masses, binding springs, and wave generators. Some observations concerning phonons in nanostructures are made as a guide to potentially application in future researches on system of bass dimensionally. In predicting future developments in the fields of phonon effects in nanostructures and phonon engineering, it is instructive to consider emerging international efforts for both nanostructures and bulk structures. Indeed, novel phonon effects in bulk materials are likely to have counterparts in nanostructures. Progress in femtosecond lasers and ultrafast spectroscopy and the continued development of novel techniques for fabricating nanostructures such as quantum dots (Empedocles, 1996) have been the basis for experimental observations of coherent oscillations of acoustic phonons in superlattices (Sun et al., 1999), damped spherical acoustic breathing modes in quantum dots (Krauss and Wise, 1997, see the supporting analysis of Stroscio and Dutta, 1999), optical phonons near the surface of bulk.

References

[1] A. Felly, F. Gagel, K. Maschke, A. Virlouvet and A. Khater, Phys.Rev.B55, 1707(1997)

[2] A. Virlouvet, A. Khater, K. Maschke, and O. Rafil, Phys.Rev.B59, 4933(1999)

[3] C. Berthod, F. Gagel and K. Maschke, Phys.Rev.B50, 18299(1994)

[4] M. Belhadi, O. Rafil, R. Tigrine, A. Khater, J. Hardy and K. Maschke, Eur. Phys. J. B15, 435 (2000)

[5] A. Khater and W. Czaja, Physica B167, 33 (1990)

[6] M. Buttiker, Y. Imry, R. Landauer, S. Pinhas, Phys. Rev. B31 (1985) 6207

[7] J. Szeftel and A. Khater, J. Phys. C: Solid State Phys., 20, 4725(1987)

[8] J. Szeftel, A. Khater, F. Mila, S. Adato, N. Auby, J. Phys. C: Solid State Phys., 21, 2113 (1988)

[9] M. Belhadi, A. Khater, O. Rafil, J. Hardy and R.Tigrine, Phys Stat Sol. (b) 228, 685 (2001)

[10] P. A. Deymier, E. Oumghar, J. O. Vasseur, B. Djafari-Rouhani and L. Dobrzynski, Progress in Surface Science, Vol 53, Nos 2-4 pp. 179-186 (1997)

[11] H. Grimech and A. Khater, Surf. Sci. 323, 198 (1995)

[12] E.A. Moujaes, A. Khater, M. Abou Ghantous, J. Magn. Magn. Mater 391 (2015) 49.

[13] V.L. Moruzzi, Phys. Rev. Lett 57 (1986) 2211 ; V. L. Moruzzi et al., Phys. Rev. B 34, 1784 (1986); V. L. Moruzzi et al., Phys. Rev. B 38, 1613 (1988).

[14] G.Y. Guo, H.H. Wang, Chin. J. Phys 38 (2000) 949.

[15] B. Heinrich, et al., J. Vac. Sci. Technol. A 4 (1986) 1376 ; J. Cryst. Growth 81, 562 (1987).

[16] Z. Q.Wang, Y.S. Li, F. Jona, P.M. Marcus, Solid State Commun 61 (1987) 623.

[17] B. Heinrich, et al., Phys. Rev. B 38 (12) (1988) 879.

[18] J.A.C. Bland, et al., J. Magn. Magn. Mater. 93 (1991) 331.

[19] N.B. Brookes, A. Clarke, P.D. Johnson, Phys. Rev. B 46 (1992) 237.

[20] Z. Celinski, et al., J. Magn. Magn. Mater. 166 (1997) 6.

[21] A. Hashibon, P. Schravendijk, C. Elsaesser, P. Gumbsch, Philos. Mag. 89 (2009) 3413.

[22] J.I. Lee, S.C. Hong, A.J. Freeman, C.L. Fu, Phys. Rev. B 47 (1993) 810.

[23] T. Lin, et al., Phys. Rev. B 59 (13) (1999) 911.

[24] A. Khater, G. Le Gal, T. Kaneyoshi, Phys. Lett. A 171 (1992) 237.

[25] A. Khater, M. Abou Ghantous, J. Mag. Mag. Mat 323 (2011) 2717.

[26] V. Ashokan, M. Abou Ghantous, A. Khater, J. Mag. Mag. Mat 396 (2015) 16.

[27] V. Ashokan, M. Abou Ghantous, D. Ghader and A. Khater, J. Mag. Mag. Mat 363(2014).

[28] T.G. Dargam, R.B. Capaz, B. Koiller, Braz. J. Phys. 27/A (1997) 299–304.

[29] L. Bellaiche, D. Vanderbilt, Phys. Rev. B 61 (2000) 78